

Integration of contact elements in RGIB-module of the finite element software “CESAR-LCPC”: Application to concrete structures affected by internal swelling reactions

O. Omikrine-Metalssi & V.-D. Le
Université Paris-Est, Paris, France

J.-F. Seignol
Laboratoire Régional des Ponts et Chaussées (LRPC) de Clermont-Ferrand, France

S. Rigobert, P. Humbert & F. Toutlemonde
Université Paris-Est, Paris, France

ABSTRACT: A significant number of existing concrete dams are at present deteriorated by chemo-mechanical processes known as internal swelling reactions (ISR). These pathologies, which include delayed ettringite formation as well as alkali-aggregate reactions, are responsible for cracking and expansion of the material which lead to degradation of structures behaviour. The chemo-mechanical modelling of these phenomena is already elaborated by considering the influence of temperature and humidity in the development of expansion. This modelling is valid only for continuous media. In order to widen the domain of modelling applicability, this paper describes a novel procedure for modelling displacement discontinuities in ISR-affected concrete structures, mainly to take into account two phenomena: firstly the modelling of the isolated cracks opening that result from interactions between pathology and mechanical behaviour of the structure, and secondly, the evaluation of the potential efficiency of stress release (e.g. sawing of dams), the procedure of which consists in the creation of cutting lines in the structure for release of excessive compressive stresses, reclosing of the cut being a result of subsequent swelling. The elaborated model, aimed to possibly combine contact elements and non-linear coupled models of durability mechanics related to ISR modelling, was applied to the 3D simulation of ISR in an example of simple gravity dam. Displacements and stresses at the contact elements zone were computed and compared with results of the dam computations without contact elements. The results show that the creation of cutting lines in the dam studied leads to decrease of the stresses in the structure, which confirms a favourable effect of this stress release technique in order to deal with ISR affected structures.

1 INTRODUCTION

Internal swelling reactions (ISR) can affect the long-term durability of concrete structures more particularly hydraulic concrete structures by causing cracking and expansion of the material. These pathologies mainly consist in alkali-aggregate reaction (AAR) and/or delayed ettringite formation (DEF). The Alkali-Silica Reaction (ASR) is a reaction which occurs over time in concrete between the highly alkaline cement paste and reactive non-crystalline silica, which is found in many common aggregates. This reaction causes the expansion of the altered aggregate by the formation of a swelling gel of Calcium Silicate Hydrate (CSH). This gel increases in volume with water and exerts an expansive pressure inside the material, causing loss of strength of the concrete, finally leading to its failure. Meanwhile

delayed ettringite formation (DEF) consists in ettringite crystallization within concrete after hardening is substantially complete, and in which no sulphates come from outside the cement paste. It may occur in materials that have been subjected to temperature above about 65°C and to high humidity.

The occurrence of these two phenomena in several concrete structures in the last years worldwide has pointed out the need for improvement of preventive measures to inhibit these reactions in affected structures. Moreover, prediction of concrete expansion and degradation and assessment of efficiency and periodicity of rehabilitation operations are crucial points for existing affected structures.

Several types of models to simulate the behaviour of structures affected by (ISR) have been presented in the literature (Léger *et al.* 1996, Ulm 1999 for ASR and Zhang *et al.* 2002, Brunetaud 2006, Heinz

& Ludwig 1987, Garboczi 1997 for DEF). However, in this study, we improved models proposed by Li *et al.* (2004) for ASR and Baghdadi *et al.* (2007), Baghdadi (2008) for DEF.

The modelling of these phenomena in CESAR-LCPC Finite Element code was based on a sub program called “ALKA”, for ASR, and newly developed sub program called “RGIB” that allows modeling the behaviour of a structure affected by ASR or DEF. This program takes into account several coupled phenomena: effects of the early age thermal history, anisotropy of the imposed expansion related to the direction of concrete casting, damage resulting from cracking of the material, drying shrinkage and coupling between the expansion and the state of stresses.

Many case-studies have shown that it is necessary to model displacement discontinuities in the concrete, mainly to take into account two phenomena:

- In addition to multi-cracking, observation of isolated cracks with an important opening, resulting from interactions between pathology and mechanical stresses applied to the structure. Control of these cracks opening sometimes requires an explicit modelling.

- Among techniques available to deal with ISR affected structures, the stress release can be effective (e.g. sawing of dams). To evaluate the potential efficiency of this technique, creation of cutting lines in the structure, and reclosing of the cut as a result of subsequent swelling, need to be modelled.

In this paper, we describe the algorithm development aimed to possibly combine contact elements, which the modelling was elaborated by Richer (1985), and non-linear coupled models of durability mechanics related to ISR modelling, and we present validation and illustrative cases of simple gravity dam.

2 PRESENTATION OF SOFTWARE BACKGROUND AND DEVELOPMENTS

CESAR-LCPC is a finite element software, developed at the LCPC since 1981 (Humbert *et al.* 2005). It is a finite element general software particularly adapted to the resolution of Civil Engineering problems (structural analysis, soil mechanics, etc). It includes modules of data management, libraries of elements and computational modules. In this study, contact elements were integrated in the sub-program called “RGIB” aimed to the recalculation of structures affected by internal swelling reaction, by using an other sub-program called “TCNL” which is dedicated to solving contact calculation between two non-linear solids. The finally improved RGIB-module will especially allow modeling the “sawing treatment” of ISR-affected dams.

2.1 RGIB module

Within the framework of the methodology elaborated for the expertise of ISR-affected concrete structures (LPC 2003), a method of structures recalculation has been developed. This method consists, from the information collected on the damaged structures and from the possible additional tests on reconstituted concrete, in calibrating the parameters of the laws that constitute the model. An algorithm of resolution was designed for the recalculation of structures affected by DEF or by ASR (Baghdadi 2008). It is implemented in CESAR-LCPC as “RGIB” module (Internal Swelling Reaction in Concrete) and consists in an evolution of the existing module “ALKA” which concerns the recalculation of concrete structures affected by ASR (Li *et al.* 2004, Seignol, Dubouchet 2006).

To model the kinetics of swelling reaction in relation with its mechanical consequences the curves of deformation versus time from the free expansion tests realized in laboratory under very specific environmental conditions have been used. These expansion curves have the shape of a sigmoid which can be described mathematically by using the following Equation (Brunetaud 2006, Baghdadi 2008):

$$\varepsilon_x(t) = \varepsilon_\infty^0 \frac{1 - e^{-\left(\frac{t}{\tau_c^0}\right)}}{\left(\frac{t}{\tau_c^0} + \frac{\tau_L^0}{\delta}\right)} \left(1 + \frac{\varphi}{\delta + t}\right) \quad (1)$$

where:

ε_∞^0 : Potential of expansion,

τ_c^0 : Characteristic time,

τ_L^0 : Latency time,

φ and δ : coefficients characterizing the last pseudo-asymptotic phase of expansion.

Many results show that several factors influence the amplitude and the kinetics of the swelling induced by DEF and ASR (Brunetaud 2006, Petrov 2003). Coupling laws have to describe the relation between the parameters of the expansion law presented in the equation (1) and the environmental conditions to which the structure is subjected, whether during its construction or during its lifetime.

The experiments made by (Lawrence 1995, Petrov 2003, Fu *et al.* 1994) showed that a higher curing temperature leads to increase the amplitude of final expansion. The duration of exposure to high temperature also amplifies the phenomenon (Brunetaud 2006).

Some works on the effect of the humidity on the ISR have been made. Those of Heinz & Ludwig (1987) showed that no expansion is observed below 90% of relative humidity even after 780 days. The final expansions are higher and latency/characteristic

times are shorter when the samples are kept in the water rather than 100 % of relative humidity.

To describe the influence of the moisture content on the kinetics and the amplitude, the laws presented by Poyet (2003) have been implemented after. A sensitivity analysis is detailed in Seignol *et al.* (2006).

The adopted approach in the modelling of the chemo-mechanical coupling is based on the assumption of prescribed chemical strains superimposed to mechanical deformations (Li *et al.* 2004, Baghdadi *et al.* 2008).

2.2 TCNL module

The module “TCNL” is based on the method of penalization which was developed in CESAR for con-

tact description especially using contact elements. This method introduces a specific and variable rigidity matrix at the level of the interface because it depends on the state (open/closed) of this interface at each iteration step (Richer 1985). In practice, this matrix is taken into account by adding, in the mesh of the structure, the special contact elements along the surface of contact. The principle of resolution requires to update the rigidity matrix at each iteration step, depending on the evolution of the contact interface, but avoids its reconditioning. Normally in a linear system where degrees of freedom are created or suppressed, the rigidity matrix must be reconditioned. With this method, the number of degrees of freedom remains constant on the surface due to the presence of the matrix of penalization.

The advantage of this method is that the contact

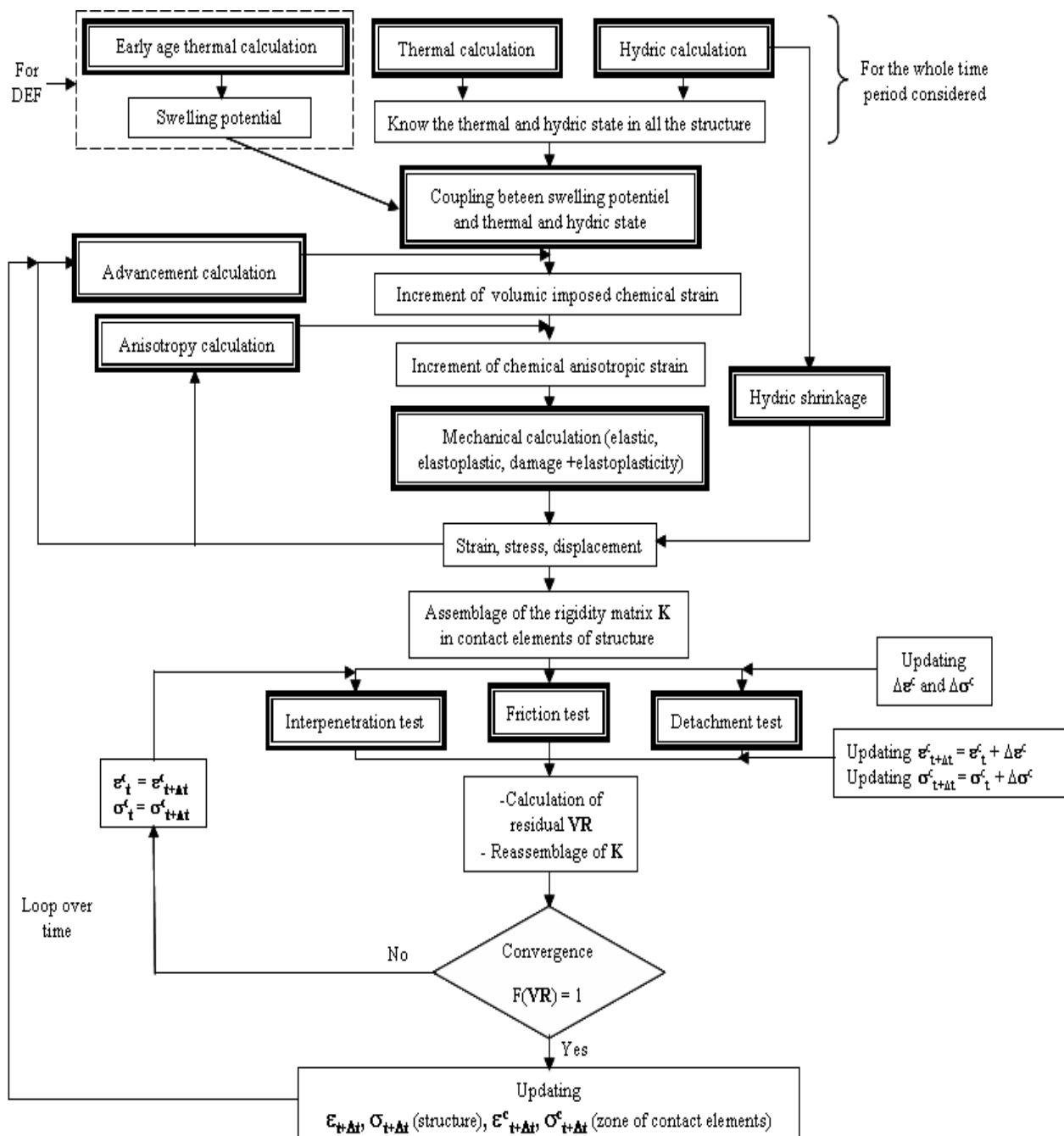


Figure 1. Resolution algorithm for RGIB-TCNL coupling problem.

elements on the potential contact surface are taken into account in the same way as the general elements of the structure, that is, through their matrix of rigidity, which is assembled in the global matrix of rigidity of the structure. These contact elements have to ensure the continuity of normal and tangential displacements in the interface. For the model used here the elements have a weak thickness but not null; the interface is then represented by a fictitious contact material and the interface elements have mechanical properties identical to the rest of the structure. The number of nodes must be compatible with that of the elements which constitute the media on both sides of the interface.

The principle of resolution consists in proceeding to a progressive loading in order to follow the evolution of the effective surface of contact. For each of these loads, we verify by an iterative process the equilibrium Equations and the criteria of contact. The changing of the effective surface of contact results in the modification of the matrix of rigidity of the contact element and thus the global matrix of rigidity. For each iteration step, we proceed to three tests: a test of non-interpenetration, a test on the normal stress and a test of friction. The first verification consists in ensuring that there is no interpenetration at the level of the inactive contact elements of the potential surface of contact. The second test consists in verifying that the normal stress in a point of the effective surface of contact is lower or equal to the tensile strength (detachment test). The last test consists in verifying that Coulomb's friction law (generally used) is satisfied at every point of the active structure area.

2.3 Coupling algorithm

The coupling algorithm of RGIB and contact elements is shown in Figure 1. Firstly, From the fields of temperature and humidity, and chemical parameters of the material, RGIB-module calculates the advancement degree of the reaction for each time step (in the case of internal sulfate attack, we have to make the early age thermal calculation first in order to have swelling potential in the structure). Then, this advancement degree is introduced into the chemo-mechanical model which leads to calculates, from a plastic or elastic law, the effects of ISR (strains, displacements, stresses). For coupling RGIB with contact elements, it is mandatory to include in the mesh the location of contact elements. These are non-active for preliminary thermal and hydric calculations and become active in the mesh during mechanical calculations. The integration of these contact elements in the calculations is made by an assemblage of their rigidity matrix and by calculating the stresses and strains at time t and $t+\Delta t$, by checking for each iteration step, the constitutive

laws that govern contact criteria (interpenetration, friction, detachment). When the calculations converge, this coupling RGIB- contact element allows to have the evolution of strains and stresses throughout the studied structure including at the contact elements zone.

3 APPLICATION TO A SIMPLE DAM STRUCTURE

3.1 Materials, mesh characteristics and parameters

An idealized part of an ASR-affected gravity dam has been used for illustrating the capacities of the developed module. The numerical simulations have been carried out, assuming concrete Young's modulus and Poisson's ratio equal to $E_c = 30000$ MPa and $\nu = 0.20$ respectively. Mass density of concrete is taken as $\rho = 2400$ kg/m³. The duration of the analysis is 50 years, assuming one year-long time steps. Total of 650 three dimensional elements and 3392 nodes in the entire model are used for finite elements calculations. The main geometric characteristics and the finite element mesh used for the simulations are shown in Figure 2. The values of the thermal and humidity fields are considered as constant. The ambient temperature and the relative humidity taken into account are of 15 °C and 100 % respectively. Temperature and humidity fields were computed using the "DTNL" module in CESAR-LCPC as shown in Figure 1 and these results are used to calculate the chemical strain in the RGIB module (Baghdadi 2008).

For the determination of the reaction kinetics (Eq. 1) we used the following values: $\tau_c = 6$ years; $\tau_L = 6$ years; $\varepsilon_\infty = 0.0015$, $\varphi = \delta = 0$. These parameters are attached to a reference temperature of 15 °C.

As for the boundary conditions, the transverse displacements were restrained on both sides, while the foundation of the dam was considered as damped (Fig. 3). The notch in the dam is represented by a contact elements zone (P1 to P6). Various constitutive laws can be envisaged for these types of elements: perfect sliding, adhesion, Coulomb friction. Each of these laws is associated to a constitutive matrix that allows to ensure the continuity on the corresponding displacements. For perfect sliding, the contact elements must only ensure the continuity of normal displacement, while for adhesion, these elements must also ensure the equality of tangential displacements. For friction, the relation between normal and shear stresses is controlled by Coulomb's law.

In the case of the studied structure, the sawing operation is assumed to have been performed after 10 years (sawing thickness is 1 cm). The mechanical behaviour of the structure can thus be compared with the reference state (without sawing). Further-

more, the reclosing of the two sides of the notch following the swelling of the dam was simulated. The results were compared with reference states either without sawing, or with a notch created from the construction time.

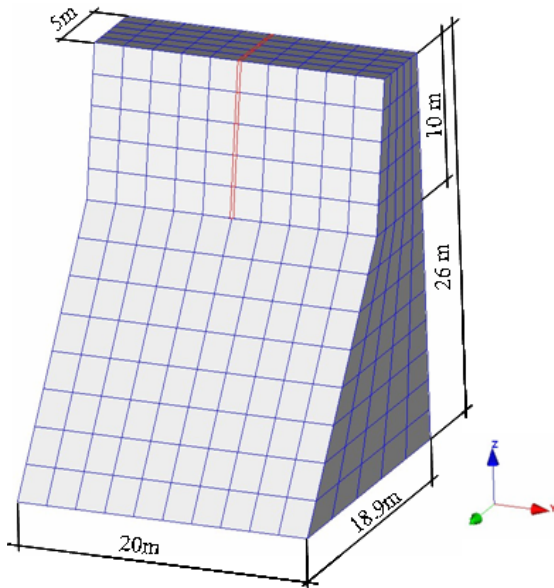


Figure 2. Geometric characteristics of the dam and finite element mesh.

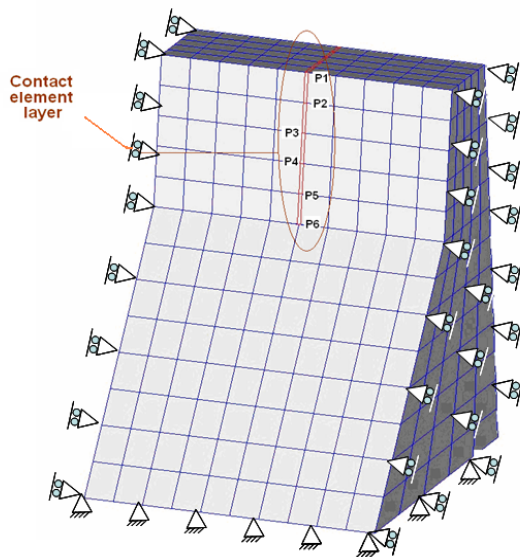


Figure 3. Contact elements and boundary conditions in the dam studied.

3.2 Results

3.2.1 Sawing after construction

Figure 4 shows the variation of vertical displacement versus time of points (P1 to P6) for the dam studied, with and without sawing on the graphs, “CE” stands for “contact elements”. This displacement increases with time and become more important when one approaches the upper surface for both cases. It stabilize after about 25 years. By comparing the results, this vertical displacement stays more important in the case without sawing (by about 5 %).

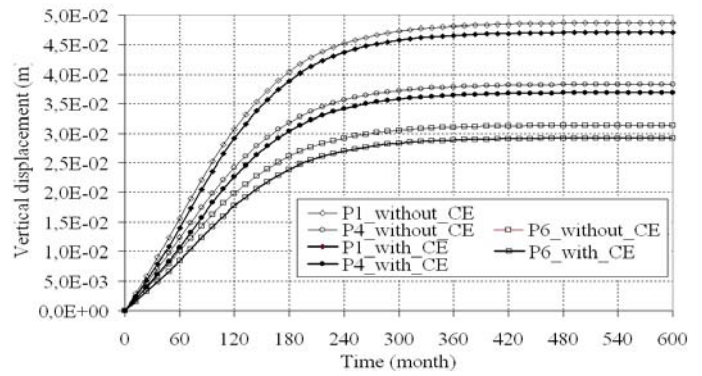


Figure 4. Vertical displacement vs. time along the sawing line (with and without sawing).

The variation of transverse displacements versus time is presented in Figure 5. The notch closes progressively from point P1 to P5 in less than 10 years. Only point (P6) is open as its transverse displacement stays lower than the value of sawing thickness. The results for the strain at this point (P6) have no physical meaning since this one is considered as a connection point between the end of the notch and the solid block which represents the base of the dam.

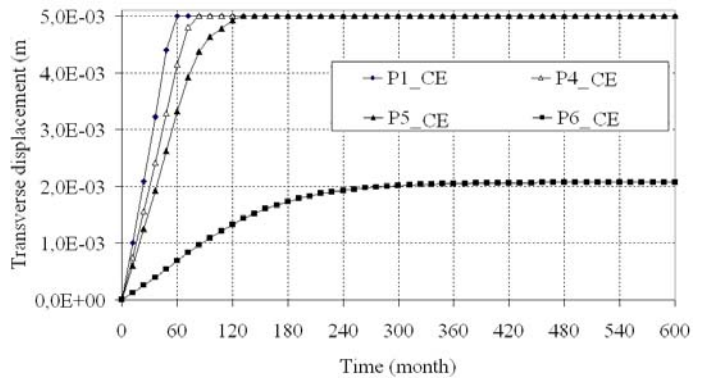


Figure 5. Transverse displacement vs. time along the sawing line after sawing.

For the variation of transverse stresses versus time, Figure 6 shows the curves for both cases: with and without sawing. For the reference case, the transverse stress increases with time until its stabilization at a value of 45 MPa. This value is roughly consistent with $E_c \cdot \epsilon_\infty^0$. While in the case of sawing, the transverse stress stays equal to zero until the progressive reclosing of the notch. Then it increases and stabilizes at values of 30 to 35 MPa. These stress values are in agreement with the theoretical values calculated at the end of the swelling. Indeed, with the sawing line thickness $e = 1$ cm made on the part of dam whose width is $L = 20$ m, the maximum transverse stress is given by (Eq. 2):

$$\sigma = E_c \cdot \epsilon_\infty^0 - E_c \cdot \frac{e}{L} \quad (2)$$

The tensile value of transverse stress at point (P6) highlights that the notch at this point stays open. As

for the strain simulations, this local stress value has no physical meaning since it corresponds to singular connection of contact and solid elements.

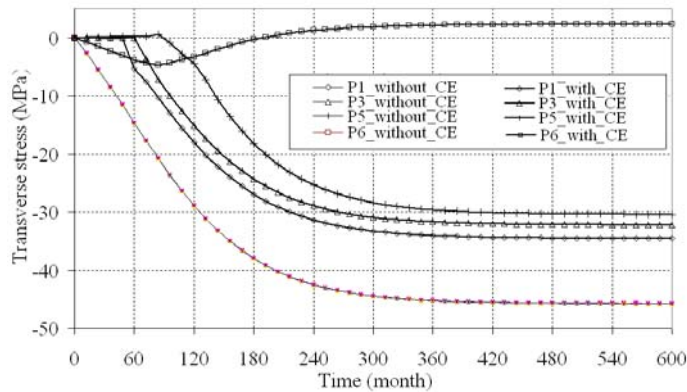


Figure 6. Transverse stress vs. time along the sawing line with and without sawing.

3.2.2 Sawing after 10 years

Figure 7 shows the variation of vertical displacement versus time of points (P1 to P6) belonging to the sawing line. Before sawing, the vertical displacements correspond to Figure 4. After sawing (after 10 years of the structure life), the displacements decrease instantaneously and increase again but stay about 5 % lower than the vertical displacements of reference case (without sawing).

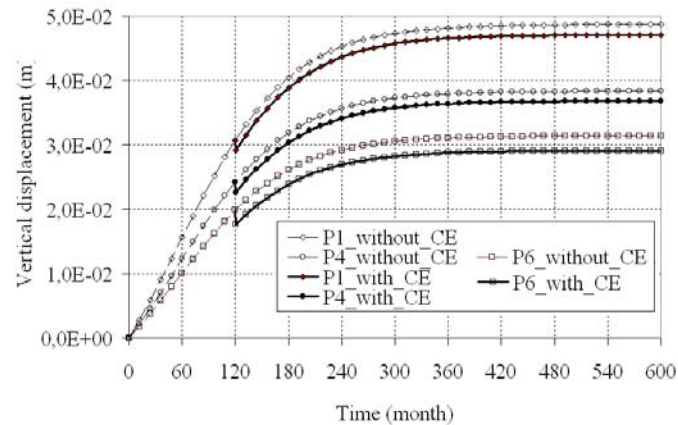


Figure 7. Vertical displacement vs. time along the sawing line before and after sawing.

Transverse displacements are displayed in Figure 8. They are zero for points (P1 to P6) until 10 years for reasons of symmetry. After sawing ($e = 1$ cm), the notch closes instantaneously and displacements on both sides of this notch take exactly the value of the sawing thickness. The notch remains open only at point P6 since the maximum displacement at this point (0.2 mm) stays lower than the value of the sawing thickness (connection point between the end of the notch and the solid blocks). Figure 9 shows the horizontal transverse displacements of the structure studied after 50 years from the construction. At this age, the transverse displacements on both sides of the notch have compensated the value of the sawing thickness.

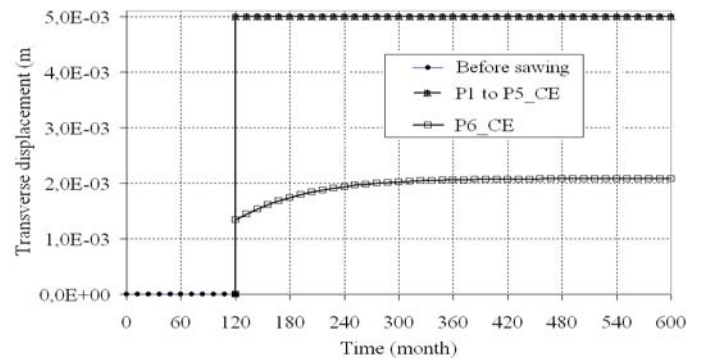


Figure 8. Transverse displacement vs. time along the sawing line before and after sawing.

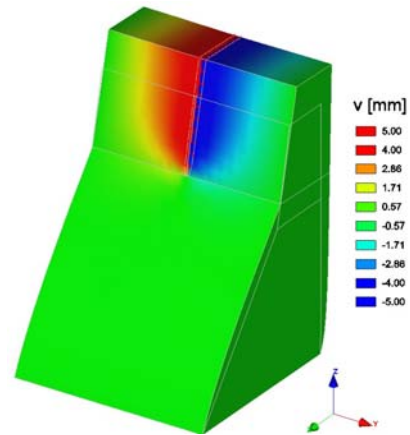


Figure 9. Transverse displacements of the dam after 50 years.

Moreover, the variations of transverse stresses versus time with and without sawing are presented in Figure 10. In fact, before sawing, the transverse stress increases with time until its stabilization at a value of $E_c \cdot \varepsilon_\infty^0 = 45$ MPa. The stresses decrease instantaneously just after sawing for all the points belonging to the sawing line, and then increase again with time until stabilization at values of 30 to 35 MPa (Eq. 2). Since the stress release is only partial, as compared to the total expansion potential, final values are similar for the cases shown in Figure 10 and Figure 6. The notch at point P6 stays open, which is highlighted by a tensile stress in this zone: this is a local artefact in this singular zone of the mesh.

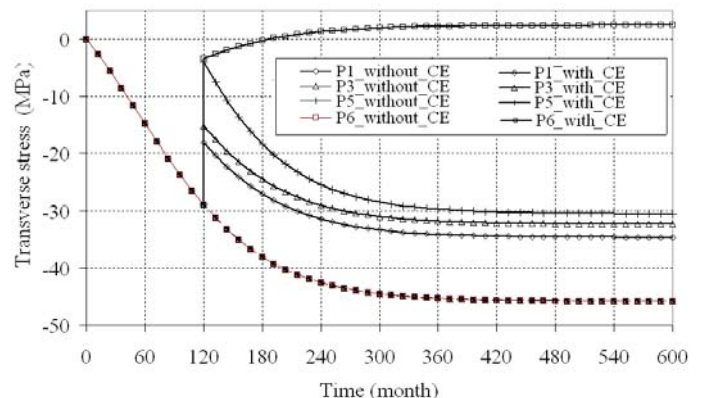


Figure 10. Transverse stress vs. time along the sawing line before and after sawing.

4 SIMULATION OF PROGRESSIVE CRACKING

Tests have been also performed for demonstrating another capacity of the developed module which is accounting for progressive cracking due to chemical swelling caused by the ISR. The numerical simulations have been performed on a simple two-dimensional case (Fig. 11) taking into account the same input parameters as for the dam calculations. This case-test, with a square shape with damped base, contains contact elements in the middle which are initially provided in the mesh. The ambient temperature and relative humidity taken into account are of 15°C and 100 % respectively.

Vertical displacements versus time of points (P1 to P4) are presented in Figure 12. The curves of all the points show an increase of this vertical displacement until its stabilisation, and it becomes more important when one approaches the upper surface of the structure studied.

Figure 13 shows the variation of transverse displacement for three different times (8, 9 and 50 years). At 8 years, the transverse displacement reaches the maximum value of about 0.86 mm, and there is still no crack. After one more year, i.e. at the 9th year, a crack appears at the contact elements

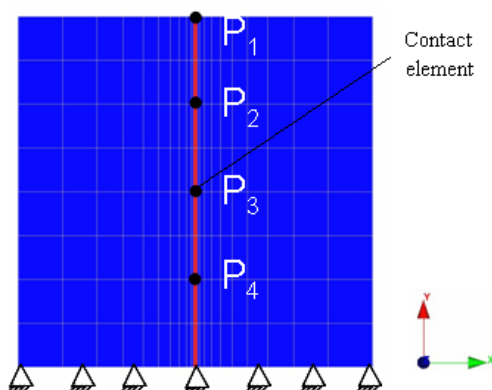


Figure 11. Contact element layer and boundary conditions in the structure studied.

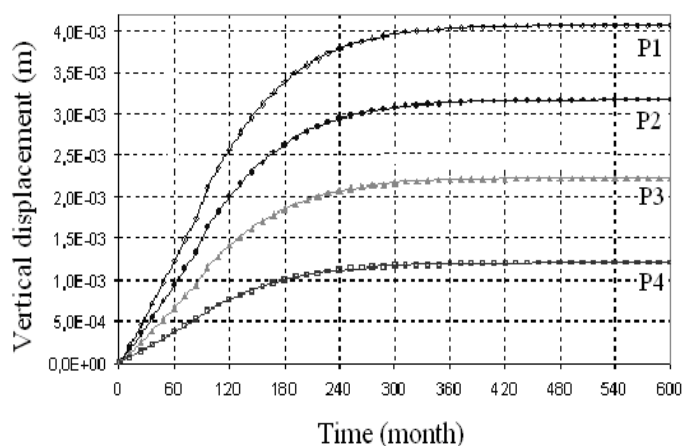
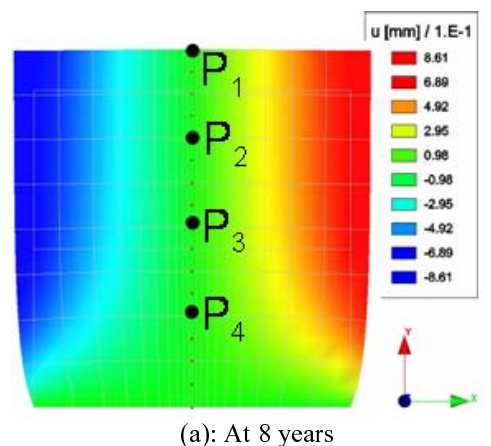
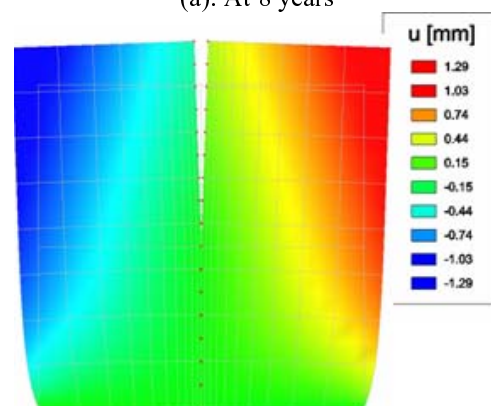


Figure 12. Vertical displacement vs. time at the contact elements after 50 years.

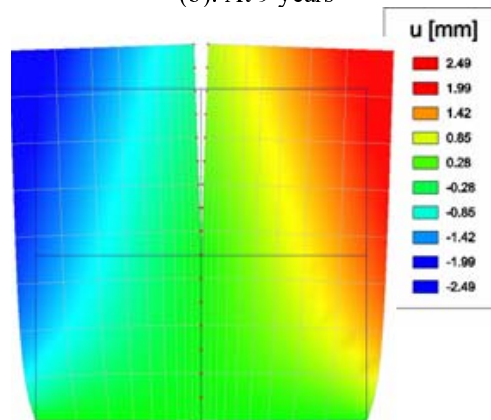
whose opening is more important at the upper surface. Thus, maximum values of transverse displacements exceed 1 mm. These values are doubled after 50 years and the opening of the crack becomes more important.



(a): At 8 years



(b): At 9 years



(c): At 50 years

Figure 13. Transverse displacements of the structure studied after 8, 9 and 50 years.

Figure 14, which presents the variation of transverse stresses versus time, highlights this crack opening. In fact, the boundary conditions allow observing a tension zone on the upper free surface (points 1 and 2). When the tensile stress reaches the tensile strength (2 MPa) after 8 years, the crack occurs engendering the stress release. This stress tends to zero for the points (P1, P2 and P3) (Fig. 14). Only the stress at point (P4) continues to increase until stabilization.

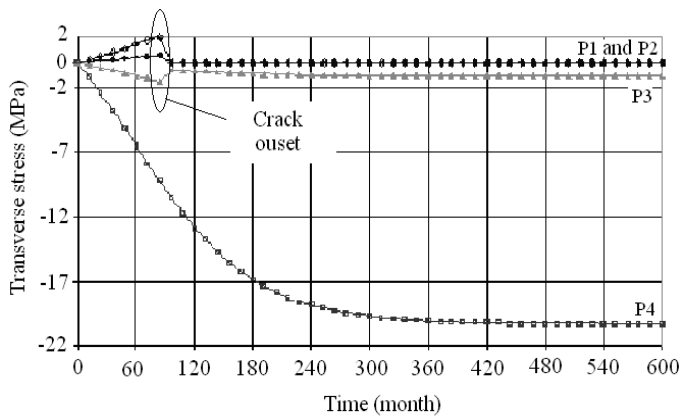


Figure 14. Transverse stress vs. time along the contact elements.

The results of the variation of transverse stresses are in perfect agreement with those of the variation of transverse displacements. In fact, the crack appears after the 8th year, which is reflected by the stress release shown in Figure 14.

5 CONCLUSION

This paper presents new functions of a Finite Element Software for modelling displacement discontinuities in concrete structures affected by Internal Swelling Reaction. It makes it possible to evaluate the potential efficiency of stress release (e.g. by sawing of dams). It can help the engineer in deciding on the choice of the number of cutting lines and their locations in the structure in order to increase its lifetime.

Furthermore, this Finite Element Software allowed to model the swelling of the structures and even if these ones are cracked. Moreover, calculations permit to follow cracks evolution.

It should be further applied to varied real-cases in support of expert engineering.

ACKNOWLEDGMENTS

The authors would like to thank STUCKY. SA (especially Mr L. Boldea) for its financial and technical support.

REFERENCES

Baghdadi, N., Toutlemonde, F., Seignol, J.F. 2007. Modélisation de l'effet des contraintes sur l'anisotropie de l'expansion dans les bétons atteints de réactions de gonflement interne, 25^{ème} rencontres de l'AUGC, Bordeaux.

Baghdadi, N., Toutlemonde, F., Seignol, J.F. 2008. Chemo-mechanical model describing the expansion due to internal sulphate attack: numerical simulation, Concrete modelling CONMOD'08, Delft, (The Netherlands), May 26-28, RILEM PRO 58, pp. 291-298.

Baghdadi, N. 2008. Modélisation du couplage chimico-mécanique d'un béton atteint d'une réaction sulfatique interne, PhD thesis, Ecole Nationale des Ponts et Chaussées, Paris, France.

Brunetaud, X. 2006. Etude de l'influence des différents paramètres et de leurs interactions sur la cinétique et l'amplitude de la réaction sulfatique interne au béton, PhD thesis, Ecole Centrale de Paris, France.

Fu, Y., Xie, P. & Beaudoin, J.J. 1994. Effect of the temperature on sulfate adsorption desorption by tricalcium silicate hydrates, *Cement and Concrete Research*, 24 (8), 1428-1432.

Garboczi, E.J. 1997. Stress, displacements, and expansive cracking around a single spherical aggregate under different expansive conditions, *Cement and Concrete Research*, Vol 27, No 4, pp. 495-500.

Heinz, D. & Ludwig, U. 1987. Mechanism of secondary ettringite formation in mortars and concretes subjected to heat treatment, Concrete durability, American Concrete Institute, K. & B. Mather, ACI SP-100, 2059-2071.

Humbert, P., Dubouchet, A., Fezans, G. & Remaud, D. 2005. CESAR-LCPC, un progiciel de calcul dédié au génie civil, *Bull. des laboratoires des ponts et chaussées*, 256-257, 7-37, LCPC, Paris.

Lawrence., C.D. 1995. Delayed ettringite formation: an issue? Material Science of Concrete. (ed. J. Skalny & S. Mindess), pp. 113-154 American Ceramic Society, Westerville, OH, USA.

Léger, P., Cote, P., Tinawir, R. 1996. Finite element analysis of concrete swelling due to Alkali-Aggregate Reaction in Dams, *Computer and Structures*, Vol. 60, pp. 601-611, 1996.

Li, K., Coussy, O. & Larive, C. 2004. Modélisation chimico-mécanique du comportement des bétons affectés par la réaction d'alcali-silice. Expertise numérique des ouvrages d'art dégradés, *Etudes et recherches des LPC*, OA43, Laboratoire Central des Ponts et Chaussées, Paris.

LPC 2003. Aide à la gestion des ouvrages atteints de réaction de gonflement interne, *Guide technique*, Laboratoire Central des Ponts et Chaussées, Paris.

Petrov, N. 2003. Combined Effect of Different Factors on Concrete Expansion due to DEF, PhD thesis, Université de Sherbrooke, Sherbrooke, Canada.

Poyet, S. 2003. Etude de la dégradation des ouvrages en béton atteints par la réaction alcali-silice : Approche expérimentale et modélisation numérique multi-échelles des dégradations dans un environnement hydro-chemo-mécanique variable, PhD thesis, Université de Marne-La-Vallée.

Richer, S. 1985. Résolution des problèmes de contact entre solides élastiques, PhD thesis, Ecole Nationale des Ponts et Chaussées, Paris, France.

Seignol, J.F. & Dubouchet, A. 2006. Cahier de développement du code de calcul ALKA, CESAR-LCPC version recherche, LCPC.

Seignol J.F., Ngo, T.T., Toutlemonde F. 2006. Modeling of the coupling between moisture and alkali-silica reaction in concrete. - "Computational Modeling of Concrete Structures", proceedings of Euro-C 2006 conference, Mayrhofen (Austria), 27-30 March, 2006, Meschke et al.eds, Taylor & Francis Group, London, pp.639-646.

Ulm F. J. 1999. Couplages thermochemomécaniques dans les bétons : un premier bilan, Laboratoire central des ponts et chaussées, *Etudes et recherches des LPC*, OA31.

Zhang, Z. Olek, J. Diamond S. 2002. Studies delayed ettringite formation in early-age heat cured mortars: 2-Characteristic of cement that may be susceptible to DEF. *Cement and Concrete Research* 32, 2002, pp.1737-1742.